Practical characterisation of the friction force for the positioning and orientation of Micro-Components.

Mickaël Paris, Yassine Haddab, Philippe Lutz, Patrick Rougeot

Practical Characterisation of the Friction Force for the Positioning and Orientation of Micro-Components

Mickaël Paris and Yassine Haddab and Philippe Lutz and Patrick Rougeot

***Abstract*— This paper deals with the description of a method for the measurement of friction force between a very small object (80 to 300 μm) and a support. The goal is to design a feeder based on controlled mechanical vibrations in order to drive microcomponents by breaking the friction force. The contact model is based on the Hertz theory and the Greenwood-Williamson multi-asperity model. The amplitude of the static friction force is measured in a clean environment with an AFM (Atomic Force Microscope) whose cantilever is placed in the vertical position. Using this setup and the modeling, we have estimated the interfacial shear stress between the microcomponent and the support.**

I. INTRODUCTION

In order to perform micro-assembly tasks, micro-assembly systems must be able to carry out three main functions: handling, joining and feeding. In the microfactory concept, feeding systems are taking a great importance to move and drive the components between and inside the assembly cells. To obtain a good efficiency, the feeding system have to be modular (at the architectural and control level) and must allow automatic control of the position and the orientation of the micro-objects.

In the literature some microsystems like conveyors and feeders based on different approaches are presented. Some of them use various fields in order to move an object or a pallet. In [1] a pneumatic conveyance is used, in [2] and [3] magnetic conveyors are developed, and in [4] an electric field is used to control the displacement step. The concept of ciliary micromotion is also developed in [5]; the ciliary micro-actuators cooperate in order to move the micro-components. Ultrasonic field is also used like [6] and [7].

One approach is to use mechanical vibration, implemented notably in the vibrating bowls [6] or step feeders where the vibrations drive a component to a particular place. However, these systems are often dedicated to particular microcomponents with sizes > 1 mm^3.

In [6], a table is moved along a vertical direction by a piezoelectric actuator, and it allows only to break the friction and surface forces. However, the positioning of the parts is obtained by the electrostatic fields produced by four electrodes.

Our objective is to design a feeder based on controlled mechanical vibrations and well adapted for very small size components by breaking the adhesion forces, very present at the small scale ($< 500\mu$m), and drive them at the right position with a very good level of precision. We propose a planar system where there is no prestressing action on the micro-component and the step is induced by using inertial force.

The displacement of the moving plate along the horizontal direction is realized by a piezo-electric stack actuator Fig. 1. It enables to get enough dynamics to break the adhesion forces and the friction forces. The result is a displacement of

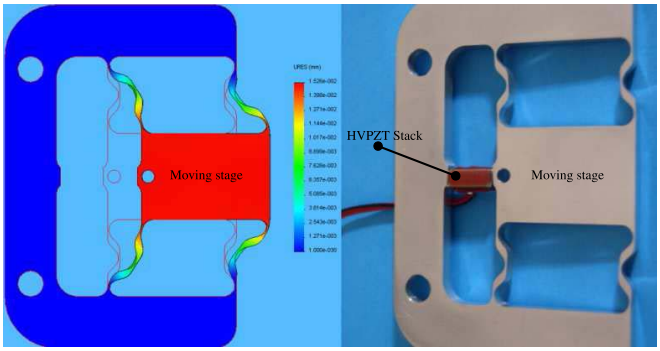

Fig. 1. Feeder by inertial force

the micro-object in the opposite direction and so, the inertial force acting on the micro-object is defined by $\sum \overrightarrow{F} = m.\overrightarrow{a}$ where F, is the tangential or inertial force, m the micro-object's mass and a the acceleration of the plate. Moreover, understanding the interactions between the surfaces of the micro-objects and the feeder is critical to control the motion. So, the plate's acceleration will be adapted for an automatic control. Friction and surface forces depend on the roughness of both surfaces. This roughness influences the contact between them. The study of roughness parameters and the contact between two flat surfaces will allow to evaluate the friction and the interfacial strengths.

II. STATE OF THE ART ON CONTACT

The static friction was first estimated by Leonardo da Vinci, Charles Augustine Coulomb, and Guillaume Amontons. The first results are known under the name of Laws of Amontons-Coulomb:

1) The force of friction is directly proportional to the applied load.
2) The force of friction is independent of the nominal area of contact.

It is in 1950 that David Tabor and Frank P. Bowden showed that the friction force F_f depends on the real area ("A_r") of contact as $F_f = \tau A_r$, where τ is the friction stress which

All authors are with FEMTO-ST Institute, UMR CNRS 6174 - UFC / ENSMM / UTBM, Automatic Control and Micro-Mechatronic Systems Department, 24 Rue Alain Savary, 25000 Besançon, France mickael.paris@ens2m.fr

is independent of the contact surface. The friction depends on three factors: the real area, the strength of interfacial bonds, and the deformation processes involved when these interfacial bonds are broken during sliding. This first model has been completed by Greenwood and Williamson [8] in order to take into account all asperities in contact between the two surfaces (Fig. 2). Each surface is characterized by the

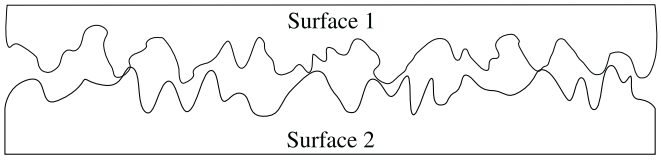

Fig. 2. Two rough surfaces in contact

geometry of its summits, which is considered as spherical, and all summits have the same radius R_i Furthermore, the height of these asperities varies randomly according to a law $\phi_i(z)$.

These two surfaces are represented by an equivalent rough surface and a perfect smooth rigid surface in contact separated by a distance d (Fig. 3). The equivalent rough surface is characterised by the shape of asperities and the height distribution. All asperity summits have the same radius R,

$$\frac{1}{R} = \frac{1}{R_1} + \frac{1}{R_2}, \tag{1}$$

where R_1 and R_2 are the mean radius of asperities of the two surfaces in contact, respectively, and their heights vary randomly following a Gaussian probability density function $\phi(z)$:

$$\phi(z) = \frac{1}{\sqrt{2\pi}\sigma} \exp\left[-0.5\left(\frac{z-\mu}{\sigma}\right)^2\right], \tag{2}$$

where σ is the standard deviation of asperity heights:

$$\sigma = \sqrt{\sigma_1^2 + \sigma_2^2}, \tag{3}$$

σ_1 and σ_2 are the standard deviation of height distribution of asperities for the two surfaces, and μ the mean height asperities of the rough equivalent surface.

The GW model considers the cumulative effect of the actions of individual local asperities, in other words, the effect of each individual asperity in contact do not affect the behavior of the nearby asperities. When an asperity is in contact, depending on its height, it is then more or less flattened and according to Hertz theory the compliance is: $\delta = z - d$.

Chang et al. [9] extended the elastic GW model into the elastic-plastic contact regime (the CEB model). In [10], the effect of adhesion was included by using the DMT model [11] for contacting asperities and the Lennard-Jones potential between non-contacting asperities. Finally a model for calculating the coefficient of friction was given in [12]. Fuller and Tabor [13] developed a theoretical model which use the JKR [14] model of adhesion with a Gaussian distribution of asperity heights. Adams and Müftü model [15], [16] includes

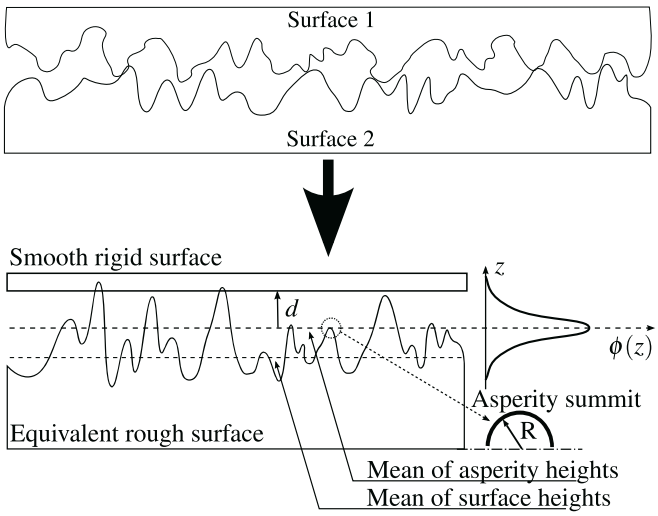

Fig. 3. GW model of contact mechanics

the effects of adhesion, and the height-dependent radius of curvature using the Maugis model and extends the Hurtado and Kim single asperity friction model [17] to a multi-asperity friction model.

III. CONTACT MODEL

For two real surfaces separated by a distance d (defined from the average height of the asperities) the number of contacting asperities n is :

$$n = N \int_d^\infty \phi(z) dz \tag{4}$$

where $N = \eta A_n$, is the number of all asperities, η the density of asperities per unit area, A_n the nominal contact area, z the height coordinate measured from the average height of asperities. The real area is defined by:

$$A_r = N \int_d^\infty A(\delta)\phi(z) dz \tag{5}$$

$A(\delta)$ being the area of a single asperity in contact and $P(\delta)$ the corresponding asperity load. So the total load is :

$$P_r = N \int_d^\infty P(\delta)\phi(z) dz \tag{6}$$

The total shear force F_r acting on the real surface, is determined by integrating the force acting on each single asperity:

$$F_r = N \int_d^\infty A(\delta)\tau\phi(z) dz, \tag{7}$$

where τ is the interfacial shear stress. As we can see, F_r depends on the area of a single asperity in contact $A(\delta)$, consequently, it depends on the choice of the model of contact.

The real surface and $A(\delta)$ depend on the load and the surface forces. These forces induce an additional surface dS on each asperity and we consider in this first work that their effects as negligible on. Thus only the load is taken into account and the contact model is based on the Hertz theory.

So $P(\delta)$ and $A(\delta)$ for a single asperity in contact is expressed by:

$$P(\delta) = \frac{4}{3}E^* R^{\frac{1}{2}} \delta^{\frac{3}{2}} = \frac{4}{3}E^* R^{\frac{1}{2}} (z-d)^{\frac{3}{2}}, \quad (8)$$

where E^* is the effective elastic modulus, and

$$A(\delta) = \pi a_\delta^2 = \pi \delta R = \pi (z-d) R, \quad (9)$$

where a_δ is the contact radius. If we combine (6) and (8) we can evaluate the separation distance d (Fig.9) since the total load is the weight of the micro-object.

$$P_r = \frac{4}{3}NE^* R^{\frac{1}{2}} \int_d^\infty (z-d)^{\frac{3}{2}} \phi(z) dz \quad (10)$$

N and R are evaluated from the scanning of the surfaces. In order to find numerically the value of d we use a function $P_r(d)$ defined piecewise on two intervals; on $[\mu, z_{max}[$, it is defined by (10); on $[z_{max}, \infty[$, it is the constant 0. z_{max} represents the highest asperity height of the equivalent rough surface. Physically, d exist only if two surfaces are in contact, then d cannot be bigger than z_{max}.

$$P_r(d) = \begin{cases} \frac{4}{3}NE^* R^{\frac{1}{2}} \int_d^{z_{max}} (z-d)^{\frac{3}{2}} \phi(z) dz & \text{if } d \in [\mu, z_{max}[, \\ 0 & \text{otherwise.} \end{cases}$$

Since we can find d, we are able to find the real contact area between the two surfaces, by using the equations (5) and (9):

$$A_r = N\pi R \int_d^\infty (z-d)\phi(z) dz \quad (11)$$

IV. FORCES MEASUREMENT

To analyse the validity of the micro-force modeling, experimental force measurements are necessary. This part deals with the presentation of the micro-force measurement system. The interactions between the micro-objects and the surface are measured by a specifically developed system called AMIS-2 (**A**FM based **MI**cromanipulation **S**ystem, *second version*).

A. Surfaces in contact

Two kinds of objects are used: micro-objects and supports. Both of them are cut in a silicon wafer. In the experiments the micro-objects are put on the support, and we study the interactions between these two objects. Two kinds of supports have been built: flat supports and supports with grooves allowing to reduce the surface by half, see Fig. 4. Let p be the period and h the step height. The nominal area between the micro-object and the support is decreased from 100% to 50%. Each micro-object is a cuboid, and the Table(I) shows their different characteristics (density of silicon : 2330kg/m^3). We are able to vary two parameters: the contact area between the micro-object and the support and the weight of the micro-objects.

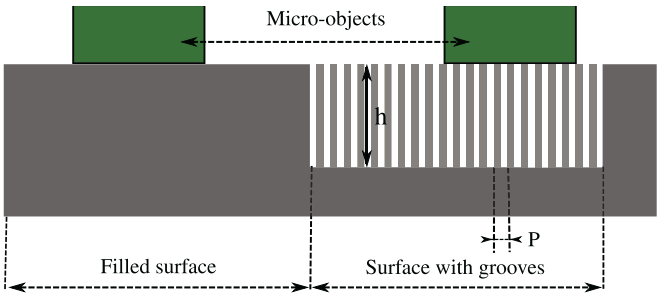

Fig. 4. Representation of the supports and the objects used.

TABLE I
QUOTATION OF MICRO-OBJECTS

Length (μm)	**width** (μm)	**height** (μm)	**Weight** (N)
80	80	50	7.3143e-09
100	100	50	1.1428e-08
200	200	50	4.5714e-08
300	300	50	1.0285e-07

B. AMIS-2 station and experimental procedures

A view of AMIS-2 is given Fig.5. This system is based on an Atomic Force Microscope and three linear micropositioning stages. These stages are used to fit the support under the AFM's cantilever and to align the micro-object with the latter. The AFM is installed in a non-conventional position. The objective is here to place the cantilever in vertical position to measure its curvature when the object is in contact. This is why, inside AMIS-2, the AFM is perpendicularly placed with regard to its "normal" position as during the scanning of a surface Fig. 6.

Different kinds of rectangular cantilevers are used to adapt the resolution according to the size of the objects and the range of the photodiode. Indeed, given that the surface of objects varies from 90000 μm^2 to 6400 μm^2, it is necessary to adapt the stiffness of the cantilever. The table II resumes the different characteristics of the used cantilevers.

TABLE II
CHARACTERISTIC OF RECTANGULAR CANTILEVERS. THICKNESS, WIDTH AND LENGTH ARE THE NOMINAL VALUES. THE RESONANCE FREQUENCY IS FOUND EXPERIMENTALLY BY THE AFM. THE STIFFNESS IS DETERMINED FROM ITS UNLOADED RESONANT FREQUENCY.

Cantilevers	Nanosensors TL-FM	Ultrasharp NSC35/AIBS
Thickness (μm)	3	2
Width (μm)	28	35
Length (μm)	225	130
Stiffness (N/m)	2.08	1.25
Resonance Frequency (kHz)	70,42	105

In order to decrease the influences of the environmental conditions, we work under a class 100 vertical laminar flow workstation, and we maintain the temperature at 25°C.

Our set-up is used to obtain experimental force curves based on the real-time measurement of the AFM cantilever bending. A force curve is a quasi-static trajectory which correspond to an "approach and depart" cycle between the

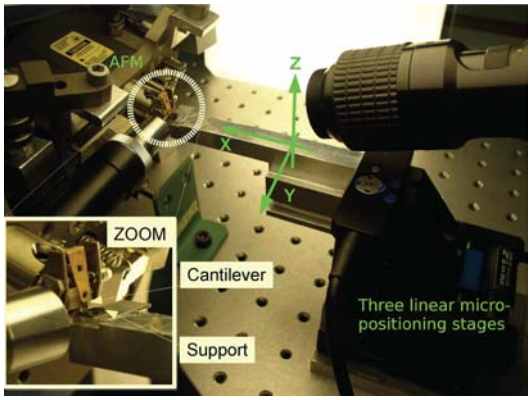

Fig. 5. AMIS-2 station

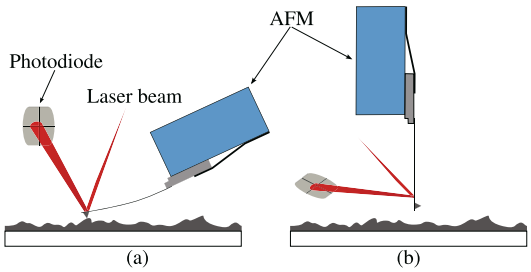

Fig. 6. AFM positions : (a) Normal, (b) Vertical

cantilever and the micro-object (in x direction) see Fig. 7. When the support and the object are aligned in y and z

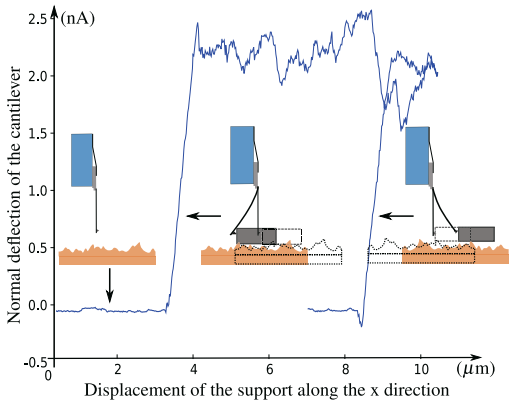

Fig. 7. Example of force curve

directions, the support is moved along the x direction. As soon as the object touches the cantilever, we observe the normal force which acts on the cantilever, until a maximal value. After that, we observe the sliding of the object on the support. The objective is to find the maximum value of the static friction, for different objects and different supports (*i.e.* roughness parameters: d, R, σ, μ, N). Before performing the evaluation of the static friction force, we perform a scan of the surface topography with the AFM (Fig.8) in order to evaluate the roughness parameters of the GW equivalent surface.

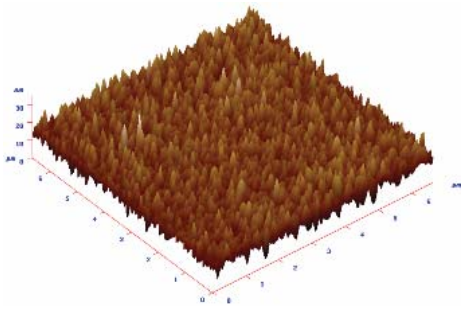

Fig. 8. Topography of silicon surface obtained using an AFM.

C. Characteristics of the equivalent surface

We define the total number of asperities for the equivalent surface, as the sum of the number of asperities for each surface. When a point resulting from the scanning is higher than its eight nearest neighbours, it is considered as an asperity summit. Thus, the mean height of the asperities for the first surface, μ_1, is calculated by :

$$\mu_1 = \frac{1}{M}\sum_{i=0}^{M-1} z_i, \tag{12}$$

where M is the number of asperities from the sample scanning and z_i their respective height. μ_2 is calculated with the same method. So μ for the equivalent surface is the average of μ_1 and μ_2. The standard deviation σ defined by (3), is obtained by estimating the root mean square (RMS) parameter S_q of each surface and is defined by

$$S_q = \sqrt{\frac{1}{M}\sum_{i=0}^{M-1} [z_i - \mu]^2}. \tag{13}$$

Equation (3) can be rewritten as:

$$\sigma = \sqrt{S_{q_1}^2 + S_{q_2}^2}. \tag{14}$$

The mean radius of asperities for each surface is obtained from a roughness profile. Each asperity is approximated by a curve fit and the mean radius is the average of all radius. As all the parameters of equation (2) and (10) are known, it is possible to calculate the separation distance d by resolving the equation (10) when $P_r(d)$ is equaled to the weight of the micro-object. Figure 9 shows the evolution of the distance d versus the load of a 300×300 micro-object put on a flat support and support with grooves. For a given load, the distance d decreases when the contact surface decreases. In fact, the number n of asperities in contact decreases, and the partial load which is supported by each of them is greater.

TABLE III
SUMMARY OF EVALUATION OF TRUE AREA

Micro-objects (μm^2)	**Real area** ($10^{-17} m^2$) flat support	**Real area** ($10^{-17} m^2$) support with grooves	**Area ratio**
300×300	4.9734	3.7833	0.76
200×200	2.2104	1.6815	0.76
100×100	0.55259	0.42037	0.76
80×80	0.35366	0.26904	0.76

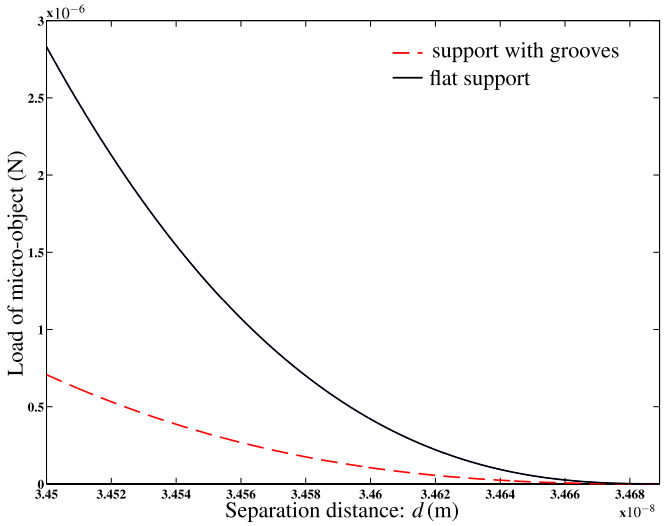

Fig. 9. Load of 300×300 micro-object vs separation distance d for a flat support and a support with grooves.

Determining d allows us to evaluate the real area. The distance d is nearly constant for any micro-object placed on the flat support ($d = 34.638$ nm). When the micro-objects are placed on the supports with grooves, we observe that $d = 34.600$ nm. In fact, their weights are so weak that they can't change significantly the separation distance. Table III resumes the obtained results. We notice a constant ratio between the true areas whatever the dimensions of the micro-objects are.

V. EXPERIMENTAL RESULTS

A. Force measurement

The micro-objects are initially placed on a flat support and the Fig.10 illustrates the force curve measured with the AFM for a 300×300 micro-object. In this example we notice a maximum value of friction force $F_r = 0.91$ μN. When the

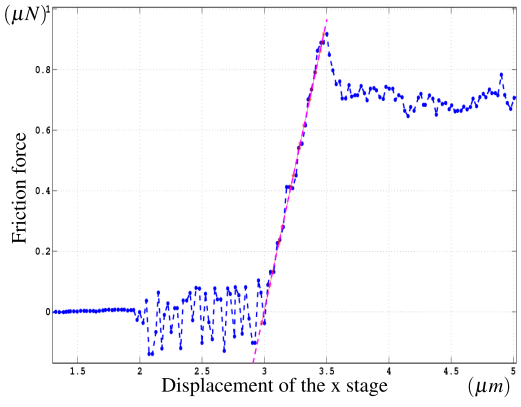

Fig. 10. Friction force curve for a 300×300 micro-object on the flat support.

micro-object is placed on the surface with grooves Fig. 11, the maximum value of the friction force decreases and in our example, $F_r = 0.708$ μN.

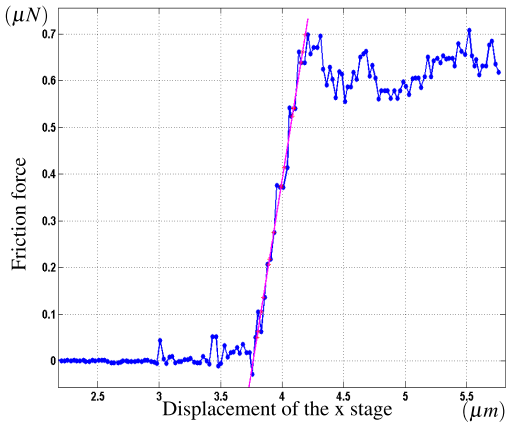

Fig. 11. Friction force curve for a 300×300 micro-object on support with grooves

TABLE IV

SUMMARY OF FRICTION FORCES MEASURES FOR A 300×300 MICRO-OBJECT PLACED ON FLAT SUPPORT AND ON A SUPPORT WITH GROOVES.

Friction forces	F_r (μN) *on flat support*	F_r (μN) *on support with grooves*	**Ratio**
	0.9759	0.7078	
	0.9174	0.6962	
Mean	0.94	0.70	0.74

We observe a diminution of the friction force amplitude when the real area decreases. In this case, the ratio between the friction force amplitudes is 0.74. This value is close to the ratio between the real areas. These first results comply the Tabor's theory between the friction force and the real area. The interfacial shear stress τ can be considered as constant at this scale. From this result we can evaluate the shear stress.

Based on the evaluation of the friction force for a 300×300 micro-objects the mean value of the interfacial shear stress is 18.75 (GPa) (see table(VI)). Other experiments have been performed using micro-objects with various sizes.

TABLE V

EVALUATION OF THE INTERFACIAL SHEAR STRESS τ FOR MICRO-OBJECTS PLACED ON A FLAT SUPPORT.

micro-objects	300	200	100	80
Real area 10^{-17}(m^2)	4.97	2.21	0.552	0.353
Mean F_r 10^{-6}(N)	0.94	0.37	0.17	0.08
τ (GPa)	19.03	16.81	25.33	22.91

Table(V) presents the results. We notice that the shear factor is between $16.81 < \tau < 25.33$ (GPa). The obtained result is $22.18 \pm 3.15 GPa$, that is equivalent to an uncertainty of 14.2%.

B. Application on the feeding system

First experiments on the feeding system have shown the validity of using a vibrating system (Fig. 1) for feeding very small components. The piezoelectric stack is supplied by a sawtooth voltage of 100 Hz and 200 V_{pp}. The obtained

TABLE VI

EVALUATION OF THE INTERFACIAL SHEAR STRESS τ FOR A 300×300 MICRO-OBJECT

micro-objects	**Real area** $10^{-17}(m^2)$ *on flat support*	**Mean** F_r 10^{-6}(N) *on flat support*	**Mean** τ (GPa)	**Real area** $10^{-17}(m^2)$ *on grooves*	**Mean** F_r 10^{-6}(N) *on grooves*	**Mean** τ (GPa)
300	4.97	0.94	19.03	3.7833	0.70	18.47

displacement for a cuboid of 500×500 μm^2, is about 3.3 μm/step. Figure 12 illustrates the presents results.

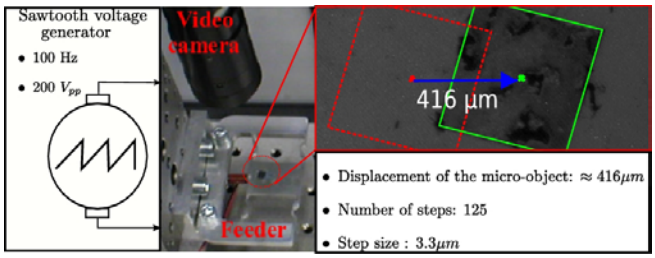

Fig. 12. Vibrating experiment.

VI. CONCLUSIONS AND FUTURE WORKS

A. Conclusions

In this work, we have presented a method to determine the friction force for a flat micro-object in contact with a flat support. This force will be used to control an inertial force feeding system. The model of contact is based on the Hertz theory and the Greenwood-Williamson multi-asperity contact theory. This first approach has permitted to evaluate the separation distance d between the surface of the micro-object and the support. Furthermore, for all the micro-objects the real contact area ratio with the flat support and the support with grooves is constant. Finally, the interfacial shear stress have been evaluated experimentally, and the results give a value of $16.81 < \tau < 25.33$ (GPa).

The experimental set up has allowed to find the maximum friction force required to move a micro-object.

B. Future Works

The evaluation of τ and d will allow to elaborate controllers for the designed feeding system. To improve our approach, we will include the effect of the adhesion forces inside the contact model by using a model based on the DMT, JKR or Maugis's theory. Moreover, experiments with other types of materials and supports will be performed.

VII. ACKNOWLEDGMENTS

This project is partially supported by the EUPASS project (Evolvable Ultra-Precision Assembly Systems: http://eupass.org).

REFERENCES

[1] Y. Fukuta *et al.*, "Pneumatic Two-Dimensional Conveyance System for autonomous Distributed MEMS," in *The 12th International Conference on Solid State Sensor, Actuor and Microsystems*, Boston, June 8-12 2003, pp. 1019–1022.

[2] H. Nakazawa, Y. Watanabe, and O. Morita, "Electromagnetic Micro-Parts Conveyer with Coil-Diode Modules," in *The 10th International Conference on Solid-State Sensors and Actuators, Transducer'99*, vol. 2, no. 1, Sendai, Japan, June 7-10 1999, pp. 1192–1195.

[3] T. Iizuka *et al.*, "A Micro X-Y-theta Conveyor by Superconducting Magnetic Levitation," in *IEEE Symposium on Emerging Technologies and Factory Automation, ETFA'94*, IIS The University of Tokyo, November 6-10 1994, pp. 62–67.

[4] F. M. Moesner and T. Higuchi, "Contactless Manipulation of Microparts by Electric Field Traps," in *Proceedings of the SPIE's International Symposium on Microrobotics and Microsystem Fabrication*, vol. 3202, Pittsburgh, October 1997, pp. 168–175.

[5] J. W. Suh *et al.*, "CMOS Integrated Ciliary Actuato Array as a General-Purpose Micromanipulation Tool for Small Objects," *Journal of Microelectromechanical Systems*, vol. 8, no. 4, pp. 483–496, December 1999.

[6] K. F. Böhringer *et al.*, "Parallele microassembly with Electrostatic Force Field," in *IEEE International Conference on Robotics and Automation (ICRA)*, Leuven, Belgium, May 16-20 1998, pp. 1204–1211.

[7] A. Haake and J. Dual, "Particle positionning by a two- or three-dimensional ultrasound field excited by surface waves," in *WCU*, Paris, 2003.

[8] J. A. Greenwood and J. B. P. Williamson, "Contact of nomally flat surfaces," in *Proceedings of the Royal Society of London*, ser. A, Mathematical and Physical Sciences, vol. 295, December 1966, pp. 300–319.

[9] W. R. Chang, I. Etsion, and D. B. Bogy, "An elastic-plastic model for the contat rough surfaces," *ASME Journal of Tribology*, vol. 109, pp. 257–263, 1987.

[10] ——, "Adhesion model for metallic rough surfaces," *ASME Journal of Tribology*, pp. 50–56, January 1988.

[11] B. V. Derjaguin, V. M. Muller, and Y. P. Toporov, "Effect of contact deformation on the adhesion of particles," *Journal of Colloid and Interface Sciences*, vol. 53, no. 2, pp. 314–326, November 1975.

[12] W. R. Chang, I. Etsion, and D. B. Bogy, "Static friction coefficient model for metallic rough surfaces," *ASME Journal of Tribology*, vol. 110, pp. 57–63, January 1988.

[13] K. N. G. Fuller and D. Tabor, "The effect of surface roughness of the adhesion of elastic solids," in *Proceedings of the Royal Society of London*, ser. A, Mathematical and Physical Sciences, vol. 345, 1975, pp. 327–342.

[14] K. L. Jonhson, K. Kendall, and A. D. Roberts, "Surface energy and the contact of elastic solids," in *Proceedings of the Royal Society of London*, ser. A, Mathematical and Physical Sciences, vol. 324, 1971, pp. 301–313.

[15] G. G. Adams and S. Müftü, "A scale-dependent model for multi-asperity model for contact and friction," *ASME Journal of Tribology*, vol. 125, pp. 700–708, 2003.

[16] ——, "Height dependent radii of curvatures in a contact and friction model," in *Proceedings of 2004 STLE/ASME Joint International Tribology Conference Long Beach*, California USA, October 24-27 2004, pp. CD–ROM Proceedings TRIB200–64 349.

[17] J. A. Hurtado and K.-S. Kim, "Scale effects in friction of single-asperity contacts. i. from concurrent slip to single-dislocation-assisted slip," in *Proceedings of the Royal Society of London*, ser. A, Mathematical and Physical Sciences, vol. 455, January 1999, pp. 3363–3383.